LA-UR-04-0919

Approved for public release; distribution is unlimited.

Title: A new approach to the reactive burn modeling of heterogeneous explosives

Author(s): Y. Horie and Y. Hamate

Submitted to: First International Symposium on Explosion, Shock Wave, and Hypervelocity Phenomena, March 15-17, 2004, Kumamoto University, Kumamoto, Japan.

A New Approach to the Reactive Burn Modeling of Heterogeneous Explosives

Y. Horie[a] and Y. Hamate[b]

Los Alamos National Laboratory, Applied Physics Division

MS F699, Los Alamos, NM 87545, USA

[a]horie@lanl.gov, [b]hamate@lanl.gov

Keywords: Solid explosives, Numerical simulation, Hot-spot modeling, Ignition, and Detonation.

Abstract. This paper discusses a new approach to building mechanistic models for shock ignition and other reactive phenomena in heterogeneous solid explosives. In the proposed approach, hot spots are treated on a unifying framework (a hot-spot cell) to integrate the three, principal response behaviors of heterogeneous energetic materials: energy localization (hot-spot formation), temperature dependent chemical reactions, and heat flow. Hot spots are treated statistically through use of a size distribution and its evolution equation. Chemical reactions start at the surface of hot spots, and the products in turn become reactants for the subsequent bulk reactions. A heat conduction equation is solved for the temperature states in the hot-spot cell. Ignition and growth of the reactive burn depend on the complex interactions of the three processes: localized energy deposition, chemical reactions (surface as well as bulk), and heat flow. Coupling of the hot-spot model to hydrodynamic flow equations is based at present on a single cell, using mass averaged mixture equations of state and a common particle velocity for the constituents. The overall model is implemented on a two-dimensional Lagrangian code called CASH. To demonstrate the predictive capability of the model, we show several exploratory calculations using RDX as a model material. They include (1) shock ignition and growth-to-detonation, (2) quenching, and (3) curved detonation in a cylindrical specimen.

1. Introduction

There are many computational models of solid explosives for large scale code calculations. Broadly speaking these models may be classified into three types. The first type is the most widely used and has several "standard" features. They are (1) single-phase overall hydrodynamic conservation equations, (2) a priori expression for the transition from the initial reactant to the final product, and (3) mass averaged thermodynamic quantities under the assumption of common pressure and common temperature. The last assumption is sometimes replaced by the adiabatic condition between the constituents. Notable examples are Forest Fire [1], Ignition and Growth [2], and JTF [3]. These models, however, are not concerned with the mechanisms of hot-spot formation. In stead, the reaction of hot spots is included as a part of the progress variable to initiate the ignition. The second type, represented by Kang et al. [4], Massoni et al. [5], and Bennett et al. [6], is an extension of the first type aimed at improving the mechanistic description of hot spot formation with focus on void collapse and frictional sliding. The progress of chemical reactions is now modeled by simplified chemical kinetics occurring on the microscale. The third type, the most complex model, replaces the overall equations by the multiphase flow equations based on a continuum mixture theory [7].

All three types share a similar mathematical scheme [8]. The differences are found in details, concerning mostly the description of hot-spot formation and distinct constituent motions. Hence the strength and weakness of each class depend on the level of description one aims to achieve. The first

type is the simplest that is designed to describe overall features such as CJ pressure and detonation speed. As a result it is most widely used for large-scale code calculations. But the models in this class are essentially phenomenological, and suffer well recognized short comings such as (1) non-physical model parameters that are difficult to determine, (2) inability to adequately describe microstructure effects such as grain size and specific area effects, and (3) the use of pressure dependent chemistry. The second type is designed to remedy the shortcomings of the first type, but they are mostly focused on a single mechanism of energy localization such as void collapse [4-6]. As discussed in [9], it is nearly inconceivable that any single mechanism will be same over the wide-ranging loading conditions. Likewise, the complexity of the third type is known to generate its own problems. Readers are referred to a excellent review article on the strength and weakness of the models based on the continuum mixture theory [10].

The new approach described in this paper belongs to the second type. However, in contrast to the existing models, we place emphasis on the development of (1) a model to unify the three princiapl mechanisms of energy localization (void collapse, shear banding, and friction) to overcome the impasse about the hot-spot formation [8], and (2) a statistical treatment of hot-spot evolution to deal with the fact that physical phenomena at the grain level are too complex to treat them directly for large scale engineering calculations. The goal is to develop a theoretical framework for building mechanistic burn models that are complex enough to describe the collective essence of microscopic events, but simple enough for practical computer calculations.

2. Unifying Hot-Spot Model

The creation of hot spots is generally accepted as fundamental to the initiation of chemical reactions in solid explosives. But in contrast to the general acceptance of the concept, there is virtually no agreement on the mechanism(s) by which the energy is localized. Examples of the mechanisms commonly discussed are spherical pore collapse, shear banding, friction, fracture, and jetting. In a typical hot-spot modeling one of those mechanisms is chosen to the exclusion of all the others. However, the likelihood of any single dominant mechanism across the wide-ranging loading conditions is doubtful and difficult to justify particularly for a complex system such as polymer-binder explosives (PBX). The result is a state of affairs characterized by Chèret as a "cold war state of non-confrontation by mutual ignorance"[8].

In the new approach we seek a détente, if one may stretch the Chèret characterization, a unifying framework in which various conceptualizations of localization may coexist. We conceived this structure, shown in Fig. 1, by abstracting the principal features of the three localization mechanisms: void collapse, shear banding, and frictional sliding. The structure in plane geometry consists of the three elements: a space occupied by gas; a finite region of localized heating surrounded by the gas and the colder solid material with a lower or zero heating rate; and the interface between the gas and the hot spot. The gas space in this model could be viewed as a space in or between explosive grains or unbonded interfaces between binder and explosive crystals. What is important in this abstraction are (1) attention is shifted from a nebulous "hot spot" to a gas-producing hot interface, and (2) the materials in the vicinity of localized heating is also a part of the conceptual hot-spot cell. In this approach energy localization is modeled parametrically by the size of the heating region and a model for heating rate as discussed in Section 3, based on the statistical treatment of "hot spots." The description of localization is not constrained by mechanism specific peculiarities. The result is a general purpose model of energy localization.

The governing equations for the new model are developed using the formulation for spherical void collapse [4,5]. We adopted their methodology for plane geometry to include key mechanisms such as viscoplastic heating, phase change, gas-phase heating, finite-rate chemical reactions, and heat transfer. The details are referred to in [9]. The principal equations are summarized in Appendix.

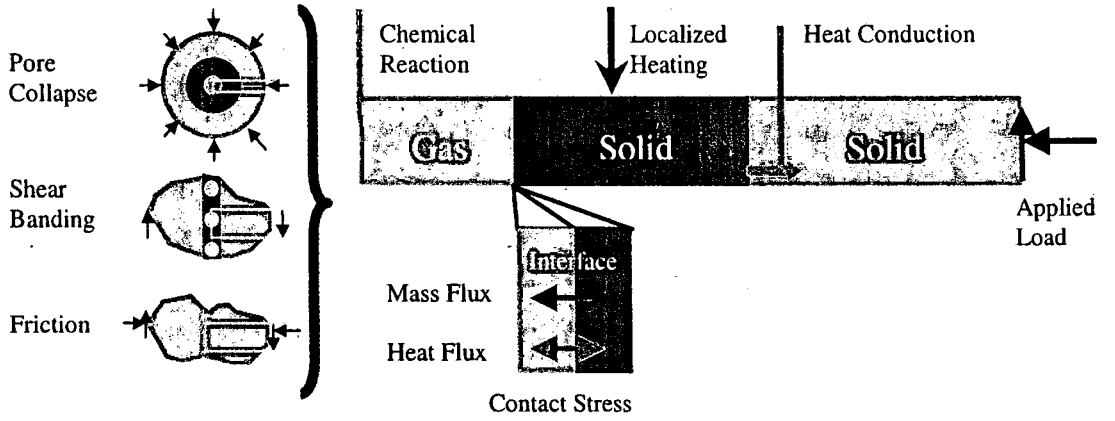

Fig. 1. A schematic of the unifying hot-spot cell consisting of gas cavity, solid-gas interface, and solid mass with a region of localized hating. Contact stress is an effect representation of interactions between grains. The left hand figures represent void collapse, shear banding, and frictional sliding schematically.

Qualitatively speaking (see Fig. 1), the model consists of solid mass, gas cavity and the interface between the two. The solid phase is assumed to be incompressible (only in the cell). Thus the particle velocity is common to all constituents, and determined by the force balance on the solid phase through the equation of motion. A new element in the derivation is the inclusion of contact stress or configuration stress that acts on the gas-solid interface. Temperatures of the solid are calculated by solving the heat conduction equation with a known heat source over the region of energy localization and heat flow from the gas phase. The latter establishes sustained reactions in the solid after the ignition. The localized energy is represented parametrically by the size of localized heating (hot spot) and a known heating rate. In this way, the difficult task of directly modeling complex grain level phenomena that depend on both loading and the state of the material is replaced by a model that projects the complex state and loading variables on the parameter space in a statistical fashion as discussed in the next section. At the solid-gas interface, conditions are imposed for the conservation of mass, momentum, and energy. The mass flux across the solid interface describes the initial phase of chemical reactions. Part of the surface reaction may involve chemical reactions depending on the temperature. In the gas cavity, the evolution of density, temperature, and chemical species is calculated by the conservation equations averaged over the gas volume. The bulk gas phase reaction is modeled by a single step Arrhenius kinetics. The equation of state for the gas is described by the Noble-Abel equation [4]. Mathematically the system consists of ten ordinary differential equations.

3. Statistical Treatment of Hot Spots

Numerical simulations of heterogeneous energetic materials at the grain level show exceedingly complex phenomena, including large fluctuations of stress and temperature over several particle diameters [11]. These fluctuations are attributed to shock interactions with materials interfaces. Hot spots are created due not only to localized plastic flow, but also shock focusing. These studies have

provided significant information to better understand physical processes in shocked heterogeneous materials, but the technique are not practical for large scale engineering calculations even with today's parallel computers . Therefore, in this study we propose a new approach for "averaging" a collection of distributed hot spots and to effectively describe the overall response behavior. The goal is to capture complexity sufficient to describe the collective essence of microscopic events, but simple enough for practical calculations. The proposed approach is schematically illustrated in Fig. 2. First we assume that hot spots in a representative volume element can be grouped gather into a two-phase medium where the gas and the solid are separated by a thin layer of aggregated hot spots. Implicitly assumed in this step is that intermediate steps in forming hot spots are not significant in burn calculations. Secondly, we normalize the total hot surface (F_A) onto a plane cross section in such a way that the motion of the plane section represents the average motion of the complex interface. The resulting hot-spot cell with all the normalized fluxes describes the cellective behavior of hot spots. This normalization adjusts not only the mass and heat transport across the interfaces, but also the rate of localized energy deposition (heating). Thus, the evolution of F_A (decribed below) defines the way we deal with the "average" effect of a hot-spot ensemble. In other mechanistic models [4,5], the overall effects are typically calculated assuming a collection of identical hot spots. In our model emphasis is placed on the importance of reacting interfaces with complex morphology (fractal like) and its equivalent representation. Also, F_A offers a means of dealing with microstructure effects on hot-spot evolution.

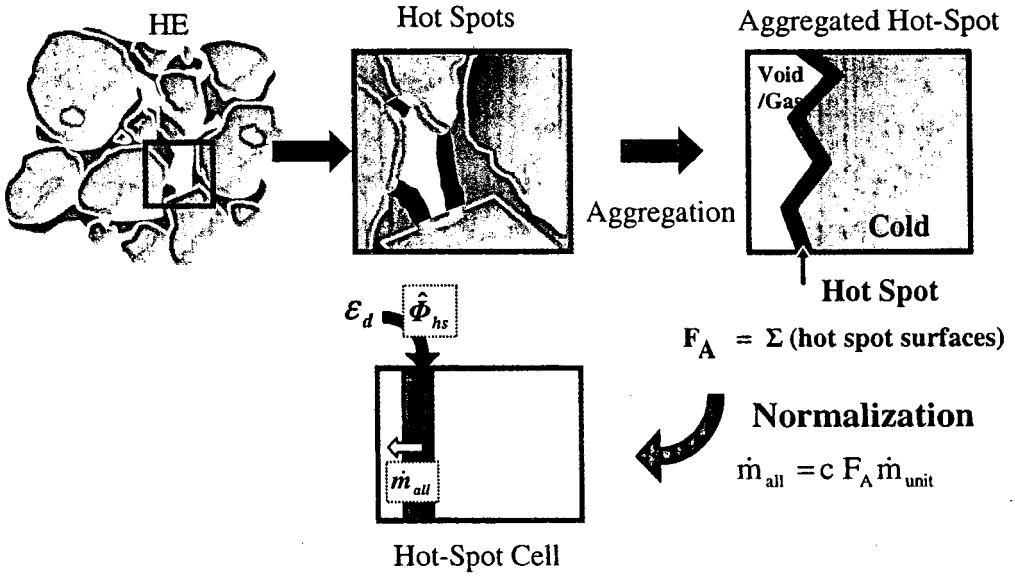

Fig. 2. Schematic illustration of modeling the collective behavior of distributed hot spots. The overall hot-spot cell is created by first aggregating hot spot surfaces, and using the total area to normalize the mass and heat fluxes onto a unit interface. The parameter c represents the size of the hot-spot cell.

The quantitiy F_A and its statistical treatment are the central ideas of the new model. Through the variable F_A we try to capture characteristics of the heterogeneous hot-spot evolution that have been revealed in detailed numerical simulation [11]. Our initial attempt to develop F_A is a variation of the Cochran model [12] and involves three assumptions. They are (1) hot-spot production rate as a linear function of the energy dissipation rate (Cochran uses a function of the rate of relative compression), (2) an exponential size distribution, and (3) a method of moments for closing the system of equations.

A rationalization for the exponential distribution function may be based, for example, on experimental and numerical observations of large force fluctuations in granular media [13]. Detail derivation is referred to in [14]. The result is a simple expression for F_A in terms of the specific dissipated energy ε_d.

$$F_A = \frac{a_{tot}}{\xi}\left(1 - \alpha \exp\left(-\xi \frac{\varepsilon_d}{\varepsilon_d^o}\right)\right), \tag{1}$$

where $a_{tot} = F_A(\varepsilon_d^o)$. Other parameters are interrelated by the following equations.

$$\xi = 1 - \alpha \exp(-\xi). \tag{2}$$

$$\frac{a_{tot}}{\xi}(1-\alpha) = a_0 = F_A(\varepsilon_d = 0). \tag{3}$$

We note that the behavior of F_A is determined by the incipient reaction area a_0 and the maximum value at $\varepsilon_d = \varepsilon_d^o$. A more advance treatment may require a stochastic formulation [11].

The normalized heat flux is determined by assuming the equivalence of adiabatic temperatures between the total hot-spot region and the normalized plane hot section. The result is given by

$$\hat{\Phi}_{hs} = \frac{M}{\delta}\frac{d}{dt}\left(\frac{\varepsilon_d}{F_A}\right), \tag{4}$$

where M is the mass of the overall cell and δ is assumed constant. The latter assumption is not required and can be relaxed if needed [6].

For multidimensional applications of the hot-spot cell, the cell needs not be identical in size and shape to the hydro cell. However, we must observe the conservation of mass and the equivalence of the volume fraction of gas products (φ_g) between the two representations. This means that we can choose the initial hot-spot cell width (c_o) as a characteristic scale parameter that is linked with F_A. For example, the grain size may be used as the basis for selecting c. Mathematically, we require the following kinematic equalities.

$$\begin{aligned}
&\rho_g^{hy} = \frac{V^{hs}}{V^{hy}}\rho_g^{hs} = \frac{(c/c_o)V_o^{hs}}{(\rho_o/\rho)V_o^{hy}}\rho_g^{hs} = \frac{c\rho}{c_o\rho_o}\rho_g^{hs},\\
&V_g^{hy} = \varphi_g V^{hy},\ \ V_g^{hs} = \varphi_g V^{hs},\\
&\rho_g^{hy}V_g^{hy} = \rho_g^{hs}V_g^{hs}, \text{ and } \rho_g^{hy}\varphi_g V^{hy} = \rho_g^{hs}\varphi_g V^{hs}.
\end{aligned} \tag{5}$$

where V^{hy}, V^{hs}, V_g^{hy} and V_g^{hs} are the volumes of the hydro and hot-spot cells, and the corresponding gas phases, respectively.

In summary, the difference between a hot-spot cell in section 2 and the global hot-spot cell is the rate of localized heating and the mass and heat trnasfer across the unit cross section. The quantities for the latter represent those for the overall effects, but normalized to a unit cross section for purpose of determining aggregate behavior. The degree of reaction for the global cell signifies the overall degree of reaction. Thus, the link to hydro calculations is simply provided by the mixture equations of state.

In the current model the treatment of the mixture equations of state is the same as that in [5] and will not be repeated here. It assumes mass averaged momentum and internal energy. Equations of state are written in a Mie-Grüneisen form as follows.

$$P = \Gamma \rho e + P^* , \tag{6}$$

where P^* is a function of density only. The assumption of partial pressure-equilibrium leads to the mixture pressure in the same form where Γ and P^* are related to the constituent quantities by

$$1/\Gamma = \varphi_g /\Gamma_g + (1- \varphi_g)/\Gamma_s , \quad \text{and} \tag{7}$$

$$P^* = \Gamma [\varphi_g P^*_g / \Gamma_g + (1- \varphi_g) P^*_s / \Gamma_s]. \tag{8}$$

where the subscripts g and s represent gas and solid respectively, and φ_g the volume fraction.

4. Model Calculations

We shall show three proof-of-concepts simulations to illustrate typical model behavior. The energy dissipation is primarily evaluated by use of the artificial viscosity [15]. However, it is found that results are similar if the dissipation is evaluated by the energy associated with the solid Hugoniot. Materials data are those for RDX in [4]. The solid Hugoniot is that listed in [16]. The product-gas is formulated using a polytropic EOS for the reference state [17]. The selection of δ =0.4 μm is based on the parametric study of ignition for RDX in [9]. The parameter ε_d° is chosen based on the dissipated energy of shock compressed RDX at the CJ pressure of 34 GPa. The material is assumed to have an initial porosity of 1%.

The first example, shown in Fig. 3, a typical ignition and growth behavior in plane geometry due to the impact shock of about 4 GPa. The shock wave is generated by a near symmetric impact where the impacting flyer is an inert solid RDX. A thin buffer is also used to avoid a false ignition at the impact end. The solutions are nearly independent of the two models of energy depositions. The features of the detonation state such as detonation speed and CJ pressure are in reasonable agreement with the handbook values [18] and the analytical solutions based on the equations of state and the sonic requirement. However, the end of chemical reactions observed in simulation was not identical to the CJ state as illustrated in Fig. 4 where the numerical paths were compared with the analytical solutions in the pressure volume plane. One possible explanation is that in simulation chemical reactions are terminated at 99.6% completion to avoid numerical impact of flame front. As seen in the figure the detonation characteristics are also dependent on mesh size. A mesh size on the order of 100 μm noticeably alters the spatial profile of shock front. Chemical reactions degrade the Neumann peak.

Athough we will not show them in the figures, detailed examinations of the early stage evolution reveal a two-stage nature of chemical revolution in solid explosives: "*First, a weak increase in the initiating shock that in turn reinforces the shock pressure down stream, then a secondary shock wave overtakes the leading shock front and results in formation of a steady detonation wave*" [18].

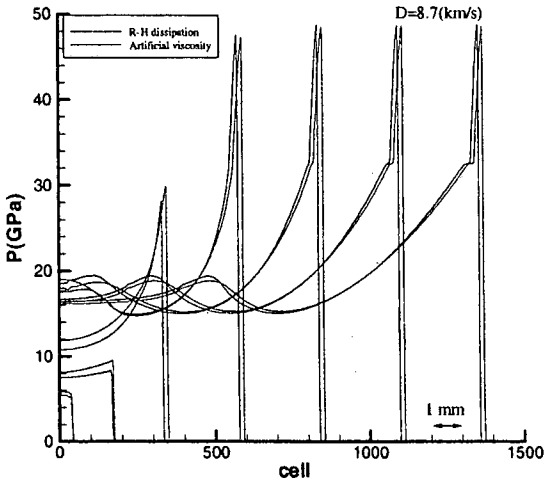

Fig. 3. Calculated growth to detonation behavior for RDX. Solutions are independent of the two modes of energy depostion.

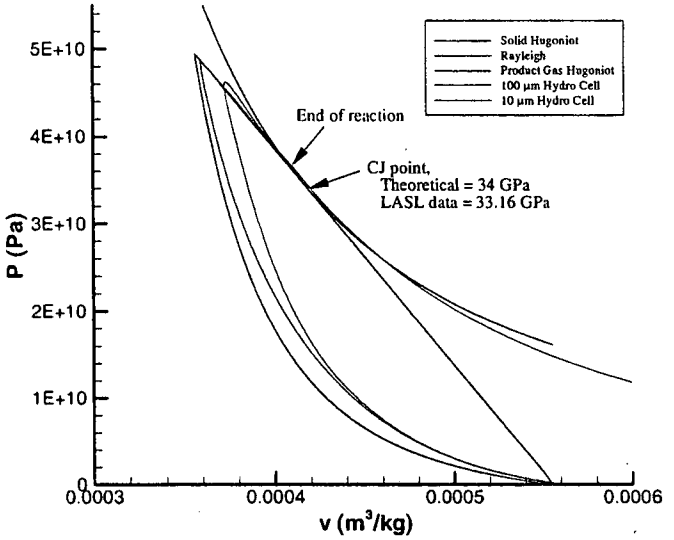

Fig. 4. Comparison of numerical paths with the analytical equations of state and the sonic CJ point. Graphically the tangent line at the end of reaction is dificult to distinguish from that at the analytical CJ point. A mesh size of 100 μm degrades the Neumann peak due to chemical reactions in the shock front.

The second example is shown in Fig. 5 where an interesting phenomenon of quenching is observed. In this example the initial shock wave is generated by a thin flyer, and rarefaction waves from the back free surface over take the the precursor shock quickly. As a result, when combustion wave reaches the precursor shock, the latter was too weak to generate a reinforced shock that is strong enough to initiate

ignition (self-sustained reactions). This is a failed example of the two-stage interpretation [18] where the reinforcement was too late to generate a strong secondary shock.

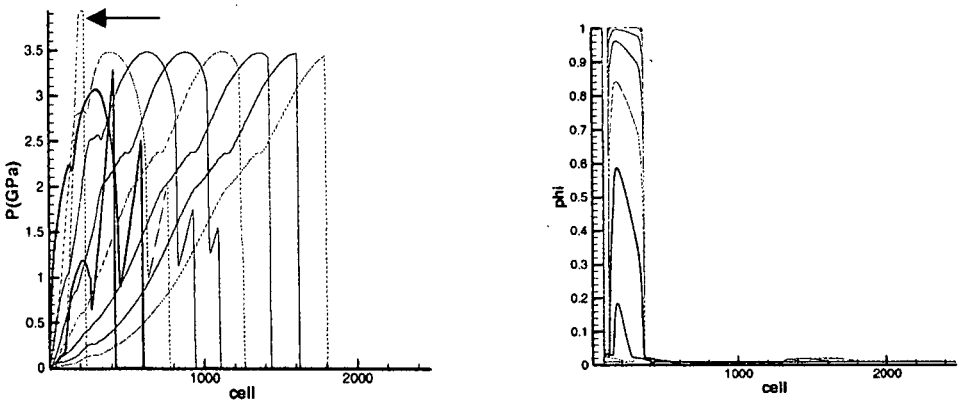

Fig. 5 Quenching of ignition by an overtaking rarefaction wave. The decay of the leading shock was too strong to produce the reinforced wave to initiate the ignition. The right hand figure shows a complete disappearance of chemical reactions.

The third example, shown in Fig. 6, is a curved detonation in a cylindrical specimen. The initiating shock in this calculation is generated by the model called "CJ Volume Burn" available on the CASH code. It generates a steady shock of about 30GPa. The detonator length is 10mm. The length of the specimen is 40 mm and has the same radius of 10 mm as the detonator. The detonation speed is 6% lower than that of the one dimensional calculation. The problem is tentatively attributed to either the product gas equation of state , the rate of energy release, or the mesh size.

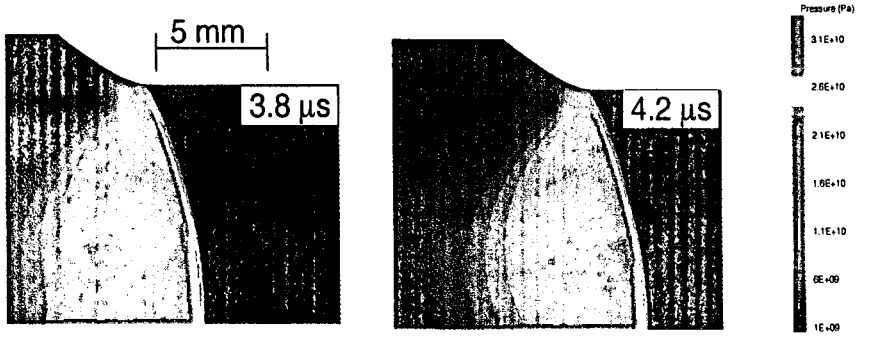

Fig. 6. Pressure contours of a curved detonation in a cylindrical specimen.

Concluding Remarks

A new theoretical framework is proposed to develop mechanistic reactive burn models for solid explosives. This approach is developed to provide a platform to deal with the heterogeneous evolution of hot spots that may result from multiple mechanisms of energy localization in the highly transient stress and temperature fields near shock fronts. Chemical processes add additional complications. In such an environment averaged field quantities are inadequate to describe initiation, failure, and growth of energetic materials.

The new approach is based on a new, planar hot spot model (cell) that involves a parametric representation of energy localization for the three principal mechanisms of energy localization and a statistical treatment of hot spot evolution. The latter assumes at present an exponential size distribution. The central concept that link distributed hot spots to the global behavior is the normalization of the total reacting surface area onto a unit section of the hot-spot cell. The evolution of the total reacting surface area based on the size distribution represents the micromechanical behavior of heterogeneous energetic materials.

Three test calculations using the material properties for RDX demonstrate the model capability in treating shock initiation, growth-to-detonation, and curved detonation at the grain level. The results are still qualitative, but the approach shows promise in developing improved and predictive models for heterogeneous reactive materials based on the statistical nature of hot spot evolution. However, there is much to be improved before the new approach will become suitable for engineering calculations. For example, the equations of state and chemical kinetics need to be tested with experimental data under a variety of conditions. Most importantly, we need to develop a hot spot distribution that include temperature and its microstructure connections.

References

[1] C. L. Mader: *Explosives and Propellant* (CRC Press, New York 1998).
[2] E.L. Lee and C.M. Tarver: Phys. Fluids Vol. 23 (1980), p.236.
[3] J.N. Johnson, P.K. Tang, and C.A. Forest: J. Appl. Phys. Vol. 57 (1985), p. 4323.
[4] J. Kang, P.B. Butler, and M.R. Baer: Comb. Flame Vol. 89 (1992), p. 117.
[5] J. Massoni et al.: Phys. Fluids Vol. 11 (1999), p. 710.
[6] J. Bennett et al.: J. Mech. Phys. Solids Vol. 46 (1998), p. 2303.
[7] M. R. Baer and J. W. Nunziato: Int. J. Multiphase Flow Vol. 12 (1987), p. 3882.
[8] R. Chèret: *Detonationm of Condensed Explosives* (Springer, New York 1992).
[9] K. Yano, Y. Horie, and D. Greening: Los Alamos National Laboratory report, LA-13794-MS (Los Alamos 2001).
[10] J. B. Bdzil et al.: Phys. Fluids Vol 11 (1999), p.378.
[11] M.R. Baer: Thermochimica Acta Vol. 384 (2002), p.351.
[12] S. Chochran: Lawrence Livermore National laboratory document, UCID-18548 (Livermore 1980).
[13] C. Thornton: KONA No.15 (1997), p. 81.
[14] Y. Horie, Y. Hamate, and D. Greening: Los Alamos National Laboratory report, LA-14008 (Los Alamos 2003).
[15] M. E. Kipp: *Proc. Eighth Symposium (Int'l) on Detonation* (Albuquerque 1985), p. 35.
[16] C-O. Leiber: Propellants, Explosives. And Pyrotechnics Vol. 25(2000), p. 288.
[17] W. Fickett and W.C. Davis: *Detonation* (Univ. of Cal. Press, Berkeley 1979).
[18] B.A. Khasinov, A.V. Attentkov, and A.A. Borisov, Chem. Phys. Reports Vol. 15 (1996).

Appendix: Mathematical Hot-Spot Model

The interface motion is described by three differential equations whose meaning can be understood intuitively,

$$\dot{a} = w_s + \frac{\dot{m}}{\rho_s} \quad , \tag{C.1}$$

$$\dot{c} = w_s \text{ , and} \tag{C.2}$$

$$\dot{w}_s = \frac{1}{\rho_s(c-a)}[\overline{p_g} + p_N - p_B + \dot{m}^2(\frac{1}{\overline{\rho_g}} - \frac{1}{\rho_s})] \quad , \tag{C.3}$$

where a is the interface position, w_s is the normal velocity of the solid phase, c specifies the external boundary of the solid phase where the global pressure p_B is exerted, and p_B is assumed to be the pressure calculated in the hydrocode. The bar above p_g and ρ_g emphasizes the fact that they are averages over the gas volume. The variable p_N is the configuration stress. Currently, it is modeled as follows:

$$p_N = -k_v\rho_s(c-a)w_s + \frac{(a_{min}/a_o)^n}{1-(a_{min}/a_o)^n}\frac{1-(a/a_o)^n}{(a/a_o)^n}p_B, (0 \le c \le c_o) \text{ ,}$$
$$= 0, (c_o \le c) \text{ .} \tag{C.4}$$

This expression contains both viscous and position-dependent parameters, and $\dot{m}$ is the rate of mass transfer across the gas-solid interface. We note that when the hot spot model is integrated into the new burn model, this quantity describes the intrinsic rate that is concerned only with local chemical kinetics. The global rate representing the mass flux for a collection of hot spots is modified by two additional functions that handle the statistics. At present $\dot{m}$ is that of Kang et al. for RDX [4] and is solely dependent on the surface temperature. Details are referred to in the original paper.

$$\dot{m}^2 = \rho_s\kappa_s T_{sa}\frac{R_u T_{sa}}{E_s}\frac{A_s\exp(\frac{-E_s}{R_u T_{sa}})}{q_s(1-G)-[c_{ps}(T_{sa}-T_o)-q_s]\ln(1/G)} \quad , \tag{C.5}$$

where G is a parameter that controls the proportion of evaporation and chemical reactions at the interface,

$$\begin{aligned} G &= 0.65 && (T_{sa} \le 700 \text{ K}) \text{ ,} \\ &= 0.69 - 2 \times 10^{-4} T_{sa} + 4.1 \times 10^{-7} T_{sa}^2 && (700 < T_{sa} < 1150 \text{ K}) \text{ ,} \\ &= 0 && (1150 \text{ K} \le T_{sa}) \text{ .} \end{aligned} \tag{C.6}$$

The average density of the gas is determined by the mass flux $\dot{m}$ and the motion of the solid phase,

$$\dot{\rho}_g = \frac{1}{a}[\dot{m}(1-\frac{\overline{\rho_g}}{\rho_s}) - \overline{\rho_g} w_s] \text{ .} \tag{C.7}$$

The surface temperature is obtained by solving the heat-conduction equation for the solid phase subject to the boundary conditions at a and c,

$$\frac{\partial T_s}{\partial t} = \alpha_s \frac{\partial^2 T_s}{\partial \chi^2} + \frac{\hat{\Phi}_{hs}}{\rho_s c_{vs}} \quad , \tag{C.8}$$

where $\hat{\Phi}_{hs}$ is the source term. The exterior boundary condition at c is assumed adiabatic, and the interior boundary condition at the solid-gas interface is the interface energy conservation equation given by

$$\kappa_s (\frac{\partial T_s}{\partial z})_a = \kappa_g \frac{T_{sa} - \overline{T_g}}{\delta_g} - \mu_s (\frac{\partial u_s}{\partial z}) u_{sa} + \dot{m}[h_{ga} - h_{sa} + a(w_s - w_{ga})] \quad , \tag{C.9}$$

where h_{ga} and h_{sa} are enthalpies of the gas and the solid at the interface, respectively.

$$h_{ga} - h_{sa} = (h^R_{ga} - h^R_{sa}) + (1-G)[\Delta]_f^{P_1} - \Delta h^R_f + (c_P^{P_1} - c_P^R)(T_{sa} - T_o)$$

$$+ \frac{1}{2}(w^2_{ga} - w^2_s) \quad , \tag{C.10}$$

$w_{ga} = w_s + \dot{m}(\frac{1}{\rho_s} - \frac{1}{\rho_g})$, and

δ_g = thermal layer thickness = a function of "a" .

The calculation of bulk gas temperature is fairly involved and is referred to in Yano et al. [9]. Only the result is listed here.

$$\overline{\rho_g} \overline{c_{pg}} \frac{d}{dt} \overline{T_g} = \frac{1}{a}\left[\kappa_g \frac{T_{sa,a} - T_g}{\delta_g} + \dot{m} c_{pg,a}\left(T_{s,a} - \overline{T_g}\right)\right] - \overline{\omega_g^R}[\Delta h_f^R - \Delta h_f^{P_2} + (c_{pg}^R - c_{pg}^{P_2})(\overline{T_g} - T_0)] + (1 - \eta \overline{\rho_g}) \frac{d}{dt} \overline{P_g} \quad , \tag{C.11}$$

where c_p stands for heat capacity and $\overline{\omega_g^R}$ is the bulk reaction rate given by

$$\overline{\omega_g^R} = -A_g \overline{Y_g^R} \overline{p_g^r} \exp(-\frac{E_g}{R_u \overline{T_g}}) \quad , \tag{C.12}$$

where A_g and E_g are a frequency factor, and an activation energy of gas-phase reaction and r is a parameter.

The kinetics of the bulk reactions are described by a set of three ordinary differential equation,

$$\overline{\rho_g} \dot{\overline{Y_g^R}} = \overline{\omega_g^R} + \frac{1}{a}\dot{m}(G - \overline{Y_g^R}) \quad , \tag{C.13}$$

$$\overline{\rho_g} \dot{\overline{Y_g^P}} = -\overline{\omega_g^R} + \frac{1}{a}\dot{m}(1 - G - \overline{Y_g^P}) \quad , \text{and} \tag{C.14}$$

$$\overline{\rho_g}\,\overline{\dot{Y}_g^I} = -\frac{1}{a}\dot{m}(\overline{Y_g^I}) \quad , \tag{C.15}$$

where superscripts R, P, and I represent reactant, product, and inert components, respectively.

The equation of state of the product gas is that of a modified ideal gas law given by

$$\overline{p_g} = \frac{\overline{\rho_g}}{1-\chi\overline{\rho_g}} R\overline{T_g} \quad . \tag{C.16}$$

The onset of the surface reaction is not necessarily equivalent to the ignition of the solid material. There has to be a continuing energy supply until such a point where there will be a sufficient amount of high-temperature reactants in the gas reservoir and a high enough surface temperature to induce self-sustained reactions both in the gas and at the solid surface. The quenching of self-sustained reactions can take place for a variety of reasons. For instance, (1) there is not enough localized energy supply, (2) the rate of localized energy supply is too slow (conducted away from the hot spot) to induce self-sustained reactions, and (3) there is not enough reactant gas, etc.